# Electroencephalogram Variability Analysis for Monitoring Depth of Anesthesia

E-mail:

Received xxxxxx
Accepted for publication xxxxxx
Published xxxxxx

## Abstract

In this paper, a new approach of extracting and measuring the variability in electroencephalogram (EEG) was proposed to assess the depth of anesthesia (DOA) under general anesthesia. The EEG variability (EEGV) was extracted as a fluctuation in time interval that occurs between two local maxima of EEG. Eight parameters related to EEGV were measured in time and frequency domains, and compared with state-of-the-art DOA estimation parameters, including sample entropy, permutation entropy, median frequency and spectral edge frequency of EEG. The area under the receiver-operator characteristics curve (AUC) and Pearson correlation coefficient were used to validate its performance on 56 patients. Our proposed EEGV-derived parameters yield significant difference for discriminating between awake and anesthesia stages at a significance level of 0.05, as well as improvement in AUC and correlation coefficient on average, which surpasses the conventional features of EEG in detection accuracy of unconscious state and tracking the level of consciousness. To sum up, EEGV analysis provides a new perspective in quantifying EEG and corresponding parameters are powerful and promising for monitoring DOA under clinical situations.

Keywords: depth of anesthesia, electroencephalogram, general anesthesia, variability analysis.

## 1. Introduction

General anesthesia is a fundamental component of modern medicine for safely performing surgical procedures on patients under loss of consciousness and analgesia [1]. Anesthesiologists recommend the best anesthesia option based on surgical types, overall health, and individual preferences of patients to precisely control the depth of anesthesia (DOA). Unfortunately, it is a big challenge for anesthesiologists to achieve adequate drug concentration but also maintain appropriate anaesthetized states due to different mechanisms of anesthetic agents and interpatient variability. A combination of different agents is administered during the maintenance of anesthesia, which is also a complicated and cognitively intensive process especially in long-term surgeries. Several studies have reported that both inadequate and excessive anesthetic may lead to bad effect on patients' safety [2-5]. Intraoperative awareness due to underdosing makes the patients suffer posttraumatic stress disorder [2, 3]. Overdosing can cause prolonged postoperative cognitive dysfunction and even increase risk of mortality [4, 5]. Therefore, there is subsequently a need to objectively and accurately monitor DOA for avoiding underdose and overdose and thus improving safety and quality of general anesthesia during surgery.

Since anesthetic drugs mainly act on the central nervous system (CNS) [6], analyzing brain activity through electroencephalogram (EEG) has attracted great attention. Currently, EEG monitoring has been widely used as a surrogate parameter to quantify either the state of well-being of the CNS or the pharmacodynamic effect of an anesthetic drug [7]. Bispectral (BIS) index (Aspect Medical Systems, USA) [8] and M-Entropy (Datex-Ohmeda, Helsinki, Finland) [9] are the most commonly used commercial methods based on EEG signal for assessment of DOA in hospitals. There are also other EEG-derived parameters developed recently. The frequency features of EEG including relative power, median frequency, spectral edge, high-order spectral analysis and so on have been proposed to assess DOA [10-12]. However, these features are highly sensitive to noise and artifacts which limits their application in clinical anesthesia. Furthermore, to calculate the spectral features, the signals need to be transformed from time to frequency domain by a discrete Fourier transform, which is a linear method. This transformation implicitly assumes that the dynamics of neural activity are stationary and linear, but do not consider the non-stationary and non-linear or chaotic behaviors in EEG signals [13]. To overcome these problems, many nonlinear analysis methods are proposed, for example, Lempel-Ziv complexity [14], detrended fluctuation analysis [15-17], fractal-scaling analysis [18], the Hurst exponent [19] and Poincaré plot [20], etc. In particular, entropies are another proposed nonlinear methods to quantify the regularity of EEG for estimating DOA, such as approximate entropy (ApEn) [21], sample entropy (SampEn) [22, 23] and permutation entropy (PeEn) [24-26]. These nonlinear features represent different aspects of EEG by providing additional information and have

 

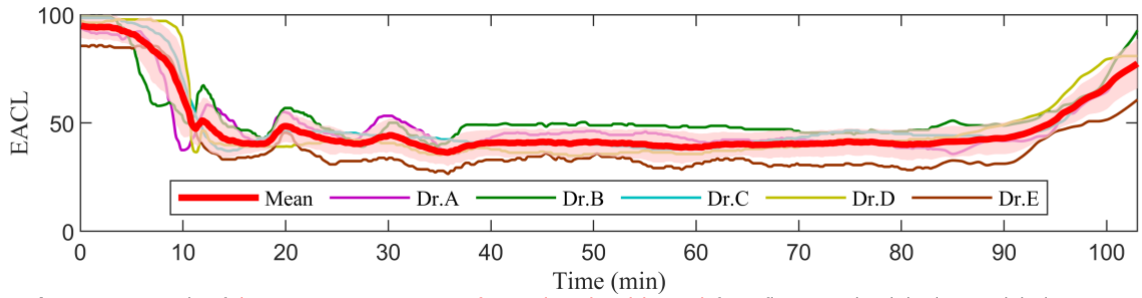


**Figure 1.** Example of the expert assessments of conscious level (EACL) from five anesthesiologists and their average.

achieved good performance for monitoring DOA. Whereas ApEn is heavily dependent on the data length and lacks relative consistency. SampEn is an improved algorithm to overcome the limitation of ApEn, but it is highly sensitive to the signal quality [27]. Thereafter, Bandt and Pompe [28] proposed PeEn based on ordinal pattern analysis of the time series. It has shown to be more robust than ApEn and SampEn due to its less sensitivity to noise and artifacts. The main disadvantage of PeEn is the paradoxical increases at the duration of burst suppression under very deep anesthesia. Moreover, the selection of parameters in these nonlinear methods is a challenge task. Although the recommend values are given [14, 15, 24], optimal parameters for each measure may be not suitable for all EEG series due to interpatient variability. To sum up, many features in diverse domains have been proposed for DOA assessment over past years, but the reliability of these monitors has been questioned in some special cases [29, 30]. There is still a necessity to explore and develop more accurate and robust methods of anesthesia assessment.

Variability analysis has been widely used in electrocardiogram (ECG) signals to measure the regulation of sympathetic and parasympathetic activities [31]. Heart rate variability (HRV) refers to the small fluctuations between consecutive heartbeat intervals. It contains a lot of information about the regulatory functions of the cardiac autonomic nervous system and cardiovascular system. Similarly, for the CNS, there exists a balance between excitation and inhibition in cortical activity, which can be affected by anesthetics through enhancing inhibitory synaptic events or depressing excitatory synaptic events [32, 33]. The increase in neuronal inhibition produces a decrease in cortical activity and in contrast excitation increases cortical activity. We expected the shifts in the balance modulated by anesthesia are accompanied by variations in EEG activity.

The purpose of this study is to open a new perspective on EEG analysis for assessing DOA. We provide a new technique called EEG variability (EEGV) analysis to characterize the fluctuations of EEG. The quasi-period interval of general signals is first defined to transform raw EEG to EEGV time series. Unlike traditional methods, EEGV measures the time between each quasi-period interval instead of raw EEG inspired by HRV method which measures the time between each heartbeat of ECG. The analyses in both time and frequency domains are given. The capability of proposed EEGV derived parameters is compared with existing EEG-based features referring to commercial BIS index and expert-labeled data during general anesthesia. It is indicated that the proposed parameters of EEGV are suitable for characterizing the sophisticated brain activity under anesthesia and perform extremely better than state-of-the-art DOA estimation methods.

## 2. Materials and methods

### *2.1 Data collection*

In this study, a total of 56 patients with American Society of Anesthesiologists physical status I-III are enrolled for analysis, 24 are male (43%) and 32 are female (57%). Age (mean ± SD) is 48.7 ± 13.8 years old ranged from 22 to 79 years, height was 162.1 ± 6.9 cm ranged from 147 to 177 cm, and weight was 64.1 ± 13.0 kg ranged from 39 to 103 kg. Seven patients are assigned to American Society of Anesthesiologists physical status I, 35 patients are assigned to II, and 14 patients are assigned to III. Written informed consents were obtained from all participants. All patients presenting surgery under general anesthesia were monitored by commercial Philip MP60 system. Before surgical operation, personal information such as age, weight, height, gender, operation type and medical history were recorded. During operation, physiological parameters like ECG, photoplethysmography, EEG, heart rate and SpO2 were monitored and collected during the whole surgery. The single-channel EEG data were collected using the BIS module and BIS sensor (3 electrode) at the sampling rate of 125 Hz. The BIS index was calculated by BIS module at a sampling rate of 0.2 Hz for DOA monitoring. After wiping the forehead with alcohol and drying, the electrodes are placed at the center of forehead, above an eye, against the patient's temple according to the instructions and configured to functions as the reference electrode, grounding electrode and EEG sensing electrode, respectively. The potential difference between reference and EEG sensing electrodes were measured as EEG signal. Each data recording started before anesthesia induction when patients were still in awake state and continued through to the end of the surgery. All EEG data are preprocessed before

subsequent analysis. The raw EEG signals are filtered by a bandpass filter within 0.5-47 Hz, which is the band considered by BIS algorithm [8]. A finite impulse response (FIR) filter instead of infinite impulse response (IIR) filter is applied to avoid disturbing the phase information in EEG. A bandstop FIR filter (59-61 Hz) is also used to remove 60 Hz power frequency interference.

At the same time, the significant events and vital signs related to anesthesia state were carefully noted on operation records by two nurses during the whole surgery, including (1) personal information: name, age, gender, weight and height, (2) physiological signal: blood pressure, heart rate, body temperature, SpO2, end-tidal carbon dioxide and minimum alveolar concentration, (3) anesthetic events: the start and end time of induction, the agents for induction and their dose, adding and reversal of muscle relaxants, type of general anesthetics, intubation, extubation, start and end time of drugs administration for maintenance, (4) surgical events: the type of surgery, the start and end time of surgery procedure and the occurrence of specific noxious stimulus, (5) clinical signs of patients: body movement, eyes closed and unusual responses, (6) other information that was possibly related to anesthesia state [34]. During the anesthesia, the induction drugs were propofol and fentanyl. Muscle relaxants were also injected. Sevoflurane (29 patients), desflurane (16 patients) or propofol (11 patients) were used for maintenance of adequate anesthesia decided by anesthesiologists. After induction and loss of consciousness, face mask (8 patients), laryngeal mask (21 patients), endotracheal intubation (26 patients), or tracheostomy (1 patient) is used to control ventilation according to the type of operation and patients' condition. Then the administration of inhalational agents (i.e. sevoflurane or desflurane) started to maintain general anesthesia by airway of laryngeal mask or endotracheal intubation. At the end of surgery, patients emerged from general anesthesia with the metabolism of drugs until to recovery of consciousness.

To evaluate the performance, a gold standard called expert assessments of conscious level (EACL) [34], which annotates the state of patients, is also provided. Five experienced anesthesiologists from National Taiwan University Hospital were asked to individually plot the score of "the state of anesthetic depth", called EACL, according to their clinical assessment on operation records of the events and vital signs, goals of therapy, and the BIS value. These selected anesthesiologists have worked for many years, so they are well trained and very skilled for administration and monitoring of general anesthesia. This course is performed after surgeries, so it is a simulation because of no contact with patients. The range of the score is settled from 0 to 100, which is the same as BIS index. A score of 100 indicates fully awake, and 0 means no brain activity. All five involved anesthesiologists assessed loss of consciousness (LOC) by BIS value below 60 which is associated with a low probability of explicit recall, and at the same time, patients were closed eyes and absence of voluntary movements. A score value ranged from 40 to 60 is defined as the suitable anesthetic depth for surgery. The score was assigned a value of less than 40 if anesthesiologists considered a patient approached a too deep anesthetic state and the doses of medications should be decreased in real surgery procedure. Contrarily, if anesthesiologists considered the depth of anesthesia was inadequate for surgical stimulation, the score was assigned a value of greater than 60. By this way, a handmade continuous-time curve ranged from 0 to 100 was plotted on recording papers to describe the conscious level of patients. Then the curves were scanned and digitized at 0.2 Hz. The annotations were made independently by themselves based on their previous experiences. So there totally comes to five EACL labeling for each individual record. Due to the inter-expert disagreement, we implement a mean value of five EACL to create an improved gold standard and increase the level of accuracy. Figure 1 gives an example of EACL from five anesthesiologists for one patient and their corresponding average.

### *2.2 EEG variability analysis*

Variability represents the fluctuation in the time intervals between periods of signal. For a given time series, to calculate the period interval, the general method is to detect the identification points of each period, such as zero-crossing points, maximum or minimum extreme points, or other special points that can be easily detected. In an ECG, R waves appear periodically and prominently, so the R-R intervals between successive R waves that detected in the QRS complex are used for HRV analysis. For EEGV analysis, inter-cycle interval (ICI) data is also required. However, EEG records the firing activity of neurons in cerebral cortex, there is no obvious point for cycle recognition to define EEGV analysis. When analyzing the characteristics of white noise signals based on empirical mode decomposition method, Wu *et al.* [35] determined the average period of intrinsic mode functions by calculating the number of peaks (i.e., local maximum). Therefore, for EEGV analysis, the time interval between two adjacent local maximum or minimum is reasonable to be accepted as a cycle period of neural circuits in the CNS regulation, which we define as quasi-period of neuromodulation.

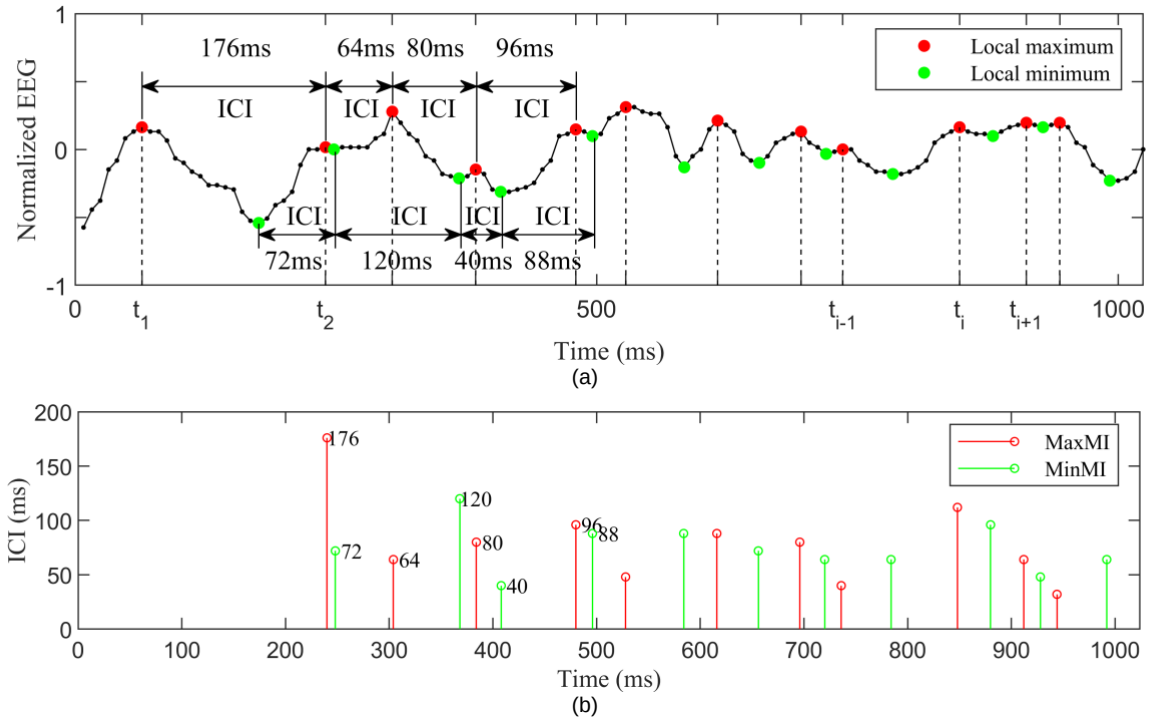


**Figure 2.** Illustrative representation of inter-cycle interval (ICI) extraction from raw EEG signal. (a) Local extrema detection and ICI definition by the time interval between successive local extrema; (b) The time series of Maximum-to-maximum interval (MaxMI) and minimum-to-minimum interval (MinMI) between successive local maxima and minima, respectively.

The algorithm for detection of local extreme points is as follows:

Given a discrete signal $x(n)$ of length $N$, the derivative of $x(n)$ is approximated by the finite difference as:

$$x'(n) = \frac{d(x(n))}{dn} = x_n - x_{n-1},\ n = 2,3,\cdots,N \quad (1)$$

At $n = n_0$, if $x'(n_0) > 0$ and $x'(n_0 + 1) < 0$, the local maximum at $n_0$ is detected. Otherwise, if $x'(n_0) < 0$ and $x'(n_0 + 1) > 0$, the local minimum is detected at $n_0$. Specially, when two or more successive points have the same value, only one extremum in the middle of the constant area is considered. For this situation, let $n_0^l$ and $n_0^r$ denote, respectively, the first and last indices of the constant area, then $n_0 = \lfloor (n_0^l + n_0^r)/2 \rfloor$, where $\lfloor \bullet \rfloor$ indicates the greatest integer function. Similarly, if $x'(n_0^l) > 0$ and $x'(n_0^r) < 0$, the local maximum at $n_0$ is detected. Otherwise, if $x'(n_0^l) < 0$ and $x'(n_0^r) > 0$, the local minimum is detected at $n_0$. Repeat these procedures until $n_0$ is the last point. An example of the local extrema detection is shown in Figure 2(a).

Thereafter, the ICI (ms) at $t_i$ can be extracted from EEG recording by time intervals between successive local extreme points in Figure 2 (a), as follows:

$$ICI_i = t_i - t_{i-1} \quad (2)$$

where $t_i$ indicates the occurrence time of $i$th maximum or minimum. Correspondingly, we define the time interval between local maxima as maximum-to-maximum interval (MaxMI) and the time interval between local minima as minimum-to-minimum interval (MinMI) as shown in Figure 2 (b). Accordingly, raw EEG signal is transformed to a series of EEGV data, defined as:

$$EEGV = \{ICI_1, ICI_2, \cdots, ICI_N\} \quad (3)$$

where $N$ is the length of EEGV extracted from EEG segments.

EEGV is analyzed by either using time-domain or frequency-domain methods. Definitions for time domain methods are as follows:

(1) AVMM (ms): the average of all ICIs of EEGV series.

$$\text{AVMM} = \frac{1}{N}\sum_{i=1}^{N} ICI_i \quad (4)$$

(2) pMMx (%): the ratio of the count of adjacent ICIs that differ by more than a threshold value of $x$ ms (i.e. $C_{ICIx}$) to the total count of all ICIs under consideration (i.e., $C_{total}$).

$$\text{pMMx} = (C_{ICIx} / C_{total}) \quad (5)$$

(3) rMSSD (ms): the square root of the mean of the sum of the squares of differences between adjacent ICIs.

$$\text{rMSSD} = \sqrt{\frac{1}{N-1}\sum_{i=1}^{N-1}(ICI_{i+1} - ICI_i)^2} \quad (6)$$

(4) SDMM (ms): the standard deviation of all ICIs.

$$\mathrm{SDMM} = \sqrt{\frac{1}{N-1}\sum_{i=1}^{N}(ICI_i - AVMM)^2} \quad (7)$$

(5) SDSD (ms): the standard deviation of successive differences between adjacent ICIs. Let $\Delta ICI_i = ICI_{i+1} - ICI_i, i = 1, 2, \cdots, N-1$ be the differences between adjacent ICIs.

$$\mathrm{SDSD} = \sqrt{\frac{1}{N-2}\sum_{i=1}^{N-1}(\Delta ICI_i - \overline{\Delta ICI})^2} \quad (8)$$

where $\overline{\Delta ICI} = \frac{1}{N-1}\sum_{i=1}^{N-1}\Delta ICI_i$ .

(6) SDAMM (ms): the standard deviation of average ICIs calculated over short time segments divided from raw signal. There will be $M$ divided segments in which $n_1, n_2, \cdots, n_M$ number of ICIs are extracted, denoted by $ICI^k$, $k = 1, 2, \cdots, M$ .

$$\mathrm{SDAMM} = \sqrt{\frac{1}{M-1}\sum_{k=1}^{M}(\overline{ICI^k} - \overline{\overline{ICI}^k})^2} \quad (9)$$

where $\overline{ICI^k} = \frac{1}{n_k}\sum_{j=1}^{n_k} ICI_j^k$ and $\overline{\overline{ICI}^k} = \frac{1}{M}\sum_{k=1}^{M}\overline{ICI^k}$ .

(7) ASDMM (ms): the average of the standard deviation of ICIs calculated over short time segments divided from raw signal.

$$\mathrm{ASDMM} = \frac{1}{M}\sum_{k=1}^{M} SD_k \quad (10)$$

where $\mathrm{SD_k} = \sqrt{\frac{1}{n_k - 1}\sum_{j=1}^{n_k}(ICI_j^k - \overline{ICI^k})^2}$ .

The frequency domain methods estimate the distribution of absolute or relative power in different frequency bands. In this context, total power (TP), median frequency (MF) and spectral edge frequency 95% (SEF) are used to reflect the overall variance, which are defined as follows:

(1) TP: the total power of ICIs within the whole frequency band.

(2) MF: the frequency at which the total power is separated into two equal 50% parts.

(3) SEF: the frequency at which 95% of the band power is presented.

The traditionally commonly used time-frequency transforms utilize a discrete Fourier transform, which often assumes evenly spaced data points in the time series. Generally, the ECG and EEG signals are sampled at a fixed sampling rate, thus they are evenly spaced with time. HRV is derived from R-R intervals (RRIs) of an ECG data by detecting R waves. EEGV is derived from MaxMIs or MinMIs of an EEG data by detecting local extrema. Because of the variation of heart rate or intervals between local extreme points, the RRI series in ECG, MaxMI or MinMI series in EEG is not uniformly spaced with time. It can be seen in Figure 2(a), the occurrence times (i.e., $t_1$, $t_2$, …, $t_i$, $t_{i+1}$) of local maxima are unequally spaced, and in Figure 2(b), the space in time (x-axis) between two adjacent MaxMI points is not equal. So HRV and EEGV can be seen as a series of unevenly spaced samples. Although interpolation and resampling can be used to obtain a regularly sampled time series, it is equivalent to a nonlinear low-pass filter, which changes the frequency components of the data and causes attenuation of high frequency. In order to overcome this problem, Lomb-Scargle (LS) periodogram method is introduced for characterizing periodicity in EEGV. For a given time series ($t_i$, $y_i$) with $N$ observations, where $i$ = 1, 2, 3, …, $N$, the LS periodogram as a function of the frequency $f$ is defined as:

$$P_{LS}(f) = \frac{1}{2\sigma^2}\left\{\frac{\left[\sum_{i=1}^{N}(y_i - \bar{y})\cos(2\pi f(t_i - \tau))\right]^2}{\sum_{i=1}^{N}\cos^2(2\pi f(t_i - \tau))} + \frac{\left[\sum_{i=1}^{N}(y_i - \bar{y})\sin(2\pi f(t_i - \tau))\right]^2}{\sum_{i=1}^{N}\sin^2(2\pi f(t_i - \tau))}\right\} \quad (11)$$

where $\bar{y} = \frac{1}{N}\sum_{i=1}^{N} y_i$ and $\sigma^2 = \frac{1}{N-1}\sum_{i=1}^{N}\left[y_i - \bar{y}\right]^2$ are the mean and variance of the time series, respectively. The parameter $\tau$ is calculated by:

$$\tan(4\pi f\tau) = \sum_{i=1}^{N}\sin(4\pi f t_i) \Big/ \sum_{i=1}^{N}\cos(4\pi f t_i) \quad (12)$$

Among the above parameters, SDAMM and ASDMM reflect longer-term variability and are suitable for a long recording, for example, longer than 24 h. For short-term recording less than 15 minutes, although it can be calculated, the results would not be meaningful. AVMM, pMMx, rMSSD, SDMM, SDSD, TP, MF and SEF measured from short-term recordings of a few seconds reflect shorter-term trends of EEGV. In general, a fixed-size sliding window is used to analyze the EEG for real-time monitoring. It is a short-term data for each calculation. Therefore, AVMM, pMMx, rMSSD, SDMM, SDSD, TP, MF and SEF are applied for real-time anesthesia assessment.

### *2.3 Statistical analysis*

Statistical analyses are performed to evaluate the proposed EEGV analysis for DOA measurement. The student's t-tests is used to determine the statistical significance of the difference between different anesthetic levels. Kruskal-Wallis test are used for testing statistically significant differences between multiple groups. All tests are two tailed with a specified statistical significance level $p < 0.05$. The Bonferroni correction is used for multiple statistical tests by multiplying the raw p-values by the number of tests. The receiver operating characteristic (ROC) analysis and area under the receiver operating characteristic curve (AUC) are

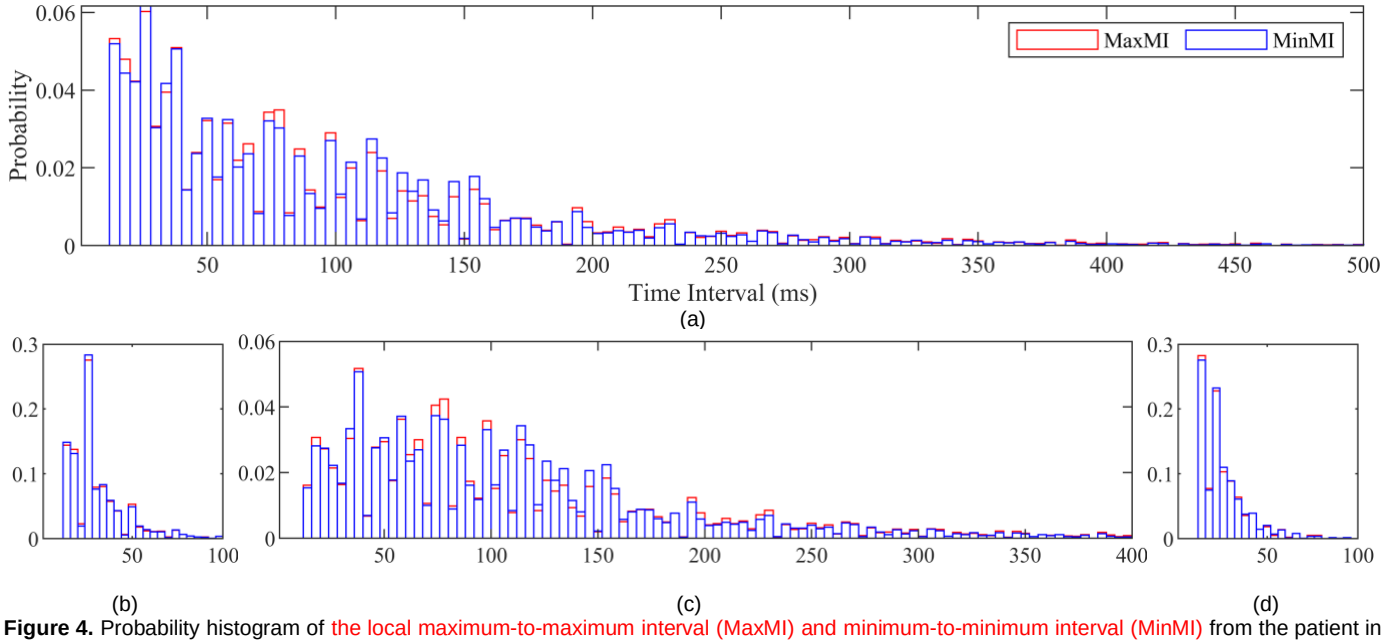


**Figure 4.** Probability histogram of the local maximum-to-maximum interval (MaxMI) and minimum-to-minimum interval (MinMI) from the patient in figure 3 during: (a) the whole general anesthesia; (b) pre-operation; (c) induction and maintenance, and (d) emergence.

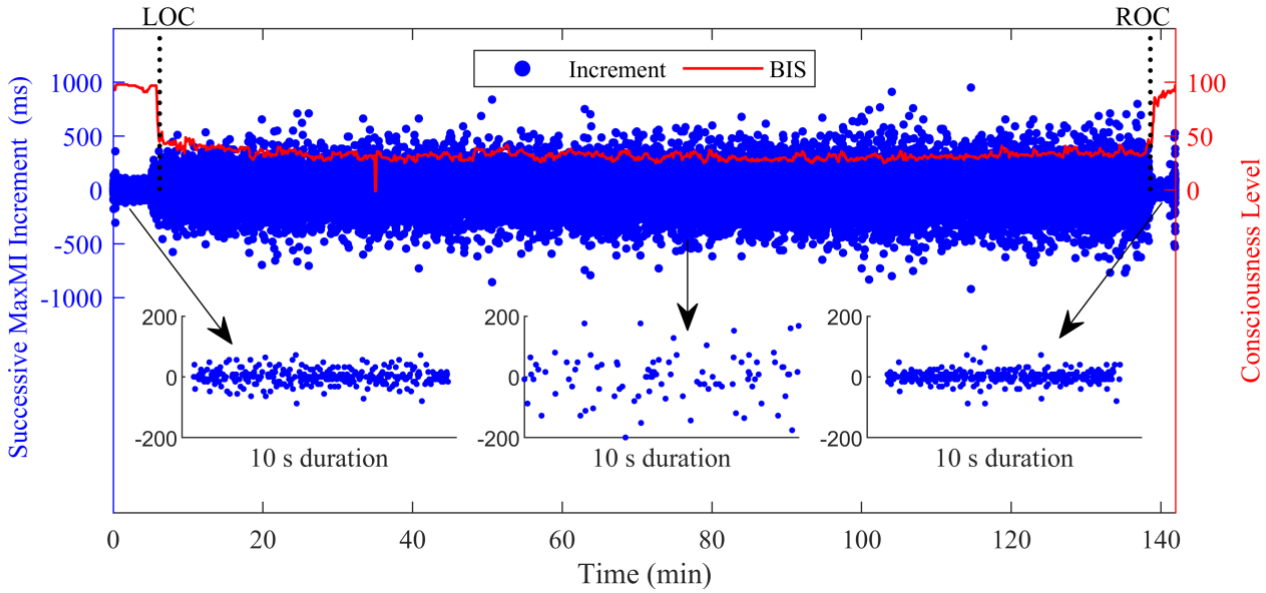


**Figure 5.** The increments in successive local maximum-to-maximum interval (MaxMI) recording in a subject during general anesthesia. The increment is calculated by subtracting the value of previous data from the current one in MaxMI series. The vertical black dot lines, from left to right, show the points of loss of consciousness (LOC) and recovery of consciousness (ROC).

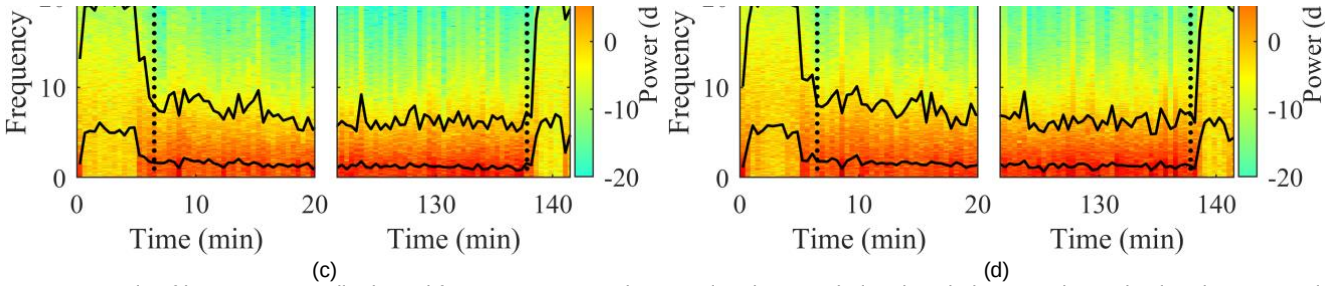


**Figure 3.** Example of how EEGV amplitude and frequency content change related to BIS during the whole general anesthesia. The scatter plots (a) and (b) show the time interval derived from the local maximum-to-maximum interval (MaxMI) and minimum-to-minimum interval (MinMI). The diagrams (c) and (d) show the spectrogram corresponding to (a) and (b), respectively, and the lower and upper black curves are the median and the spectral edge frequencies. The vertical black dot lines, from left to right, show the points of loss of consciousness (LOC) and recovery of consciousness (ROC).

## 3. Results

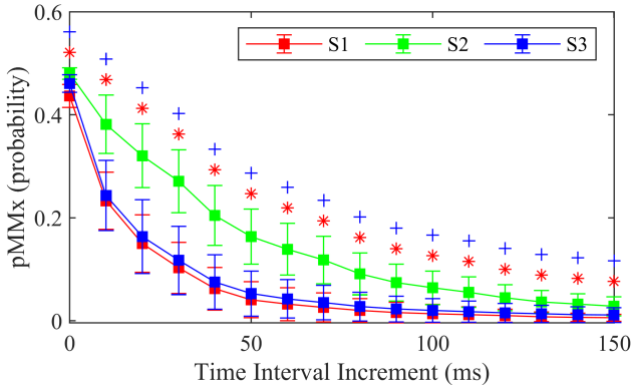


**Figure 6.** The pMMx distribution with increments between successive time intervals in 56 patients during different stages. The asterisk (*) and dagger (†) indicate significant difference of pMMx during stage 2 (S2) compared with that during stage 1 (S1) and stage 3 (S3), respectively.

**Table 1.** The Pearson's correlation coefficients between indices calculated from 1000 Hz EEG signals and those from 64 Hz, 125 Hz, 250 Hz or 500 Hz signals.

| | 64 Hz | 125 Hz | 250 Hz | 500 Hz |
|---|---|---|---|---|
| AVMM | 0.83±0.11 | 0.99±0.01 | 1.00±0.00 | 1.00±0.00 |
| pMM50 | 0.92±0.07 | 0.99±0.00 | 1.00±0.00 | 1.00±0.00 |
| rMSSD | 0.58±0.28 | 0.95±0.09 | 0.99±0.00 | 1.00±0.00 |
| SDMM | 0.55±0.29 | 0.96±0.07 | 1.00±0.00 | 1.00±0.00 |
| SDSD | 0.58±0.28 | 0.95±0.09 | 0.99±0.00 | 1.00±0.00 |
| TP | 0.76±0.12 | 0.92±0.05 | 0.99±0.00 | 1.00±0.00 |
| MF | 0.62±0.19 | 0.88±0.08 | 0.98±0.01 | 1.00±0.00 |
| SEF | 0.84±0.12 | 0.99±0.01 | 1.00±0.00 | 1.00±0.00 |

± indicates standard deviation.

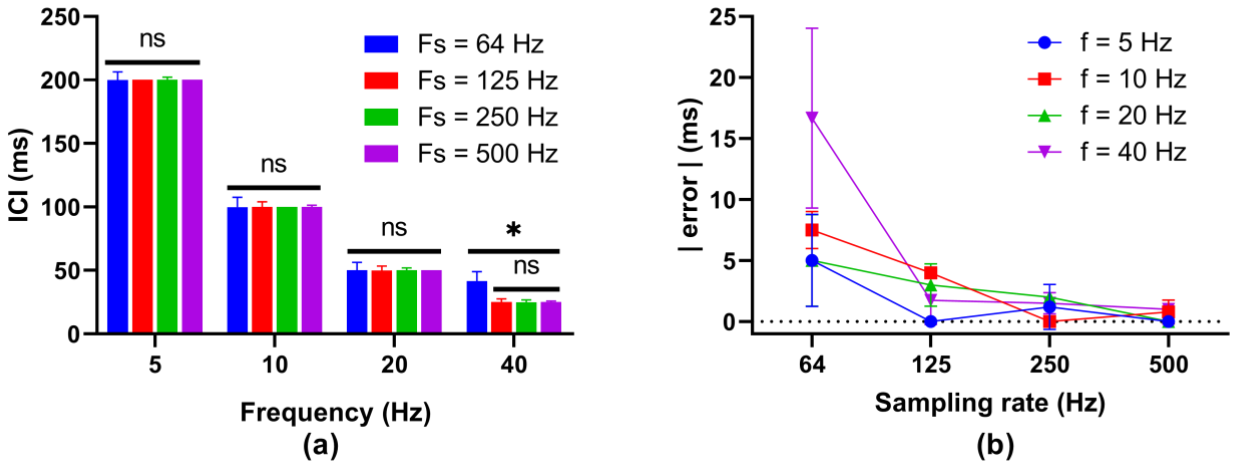


**Figure 7.** The sampling rate dependence of measured inter-cycle interval (ICI) by maximum-to-maximum interval (a) and their errors (b) from simulated sine functions with different frequencies and sampled at different frequencies. The asterisk (*) indicates significant difference between groups, while ns indicates no significant difference. Fs means sampling rate and f is the frequency of sine function.

used for assessing the discrimination performance. To further assess its accuracy in tracking the level of consciousness, the correlation with EACL and BIS is assessed by Pearson correlation coefficient. All statistical data are presented as mean ± SD.

### *3.1 Time and frequency analysis of EEGV*

The whole surgical procedure is generally divided into three periods: pre-operation, induction and maintenance, and emergence, defined as stage1 (S1) to stage3 (S3) [36]. Before induction, patients have a normal and active EEG. Then administration of a small dose of drugs induces a state of sedation, and with the dose slowly increasing, patients lose consciousness which will be maintained by a combination of anesthetic agents during the period of anesthesia. Emergence is the recovery from general anesthesia until to a fully awake state. Figure 3 presents an example of EEGV changes related to BIS during the whole general anesthesia. The spectrogram is calculated using a Hanning window of length 30 s with an overlap of 5 s points. With loss of consciousness under induction and maintenance of adequate general anesthesia, EEGV amplitude increases, and then decreases with recovery of consciousness during emergence from general anesthesia. The alterations in frequency content of the EEGV are also related to the anesthetic drug effects. Awake and emergence tends to cause the appearance of patterns at higher frequencies. On the contrary, the lower frequency patterns dominated EEGV with increasing depth of anesthesia. It also can be noted that the changes of MaxMI are almost identical to that of MinMI in both amplitude and frequency during general anesthesia. Furthermore, the probability histogram of EEGV amplitudes during different stages are shown in Figure 4. The MaxMI and MinMI have nearly the same distribution no matter on the whole general anesthesia (Figure 4(a)) or three

different stages (Figure 4(b)-(d)). In view of this, we will only focus on MaxMI for EEGV analysis in subsequent sections.

The changes between successive MaxMIs occur frequently but irregularly as shown in Figure 5. Increments as the differences between adjacent elements in a MaxMI series are calculated by subtracting the value of immediate previous element from the current one. If the current data is greater than its previous data then the increment is positive (> 0), while if the current data is less than its previous, the increment is negative (< 0). Both positive and negative increments, which are almost symmetric with respect to zero, are generated in MaxMIs. The increments during awake show a much smoother trend with only smaller amplitudes, while they have a wider range with both smaller and larger amplitudes during induction and maintenance. The incidence of larger changes in adjacent MaxMIs is measured by pMMx defined by the fraction of MaxMIs changes greater than a given threshold *x* from the preceding interval. We summarized the results by the proportion of changes exceeding different thresholds. Figure 6 shows the mean and standard deviation of pMMx distribution in 56 patients during different stages. The proportion of larger differences during unconsciousness is significantly higher than the awake and recovery values. The difference of pMMx during S2 compared with that during S1 and S3 tends to be greater at the thresholds of 30, 40 and 50 ms. These levels all clearly separate unconsciousness from consciousness state. The threshold value of 50 ms (i.e., pMM50) is selected to measure larger changes in successive MaxMI for EEGV analysis.

### *3.2 Stability under different sampling rates*

As in HRV analysis, the sampling rate directly affects the accuracy of R wave detection, which results in error in obtaining HRV parameters. Although this error can be decreased by increasing the sampling rate, an acceptable minimal sampling frequency is a better choice limited by storage space, calculation time, transmission bandwidth and so on. Theoretically, all the information can be captured at a sampling rate greater than twice the upper frequency according to Nyquist-Shannon sampling theorem. Similarly, EEGV analysis are highly dependent on the accuracy in detecting locations of local extrema.

To confirm the effect of different sampling rate on the accuracy in detection of local extrema, simulations using sine functions of different frequencies (i.e., 5 Hz, 10 Hz, 20 Hz and 40 Hz) under four sampling rates (i.e., 64 Hz, 125 Hz, 250 Hz and 500 Hz) are performed. The time length of the generated sine waves is 30 s. The means and standard deviation of ICIs extracted by MaxMI from the sine waves are shown in figure 7 (a), and the absolute errors between the measured ICI and theoretical value (i.e. period of sine function) are also calculated as shown in Figure 7 (b). The results indicate that there is no statistically significant difference between groups of 5 Hz, 10 Hz and 20 Hz under different conditions of

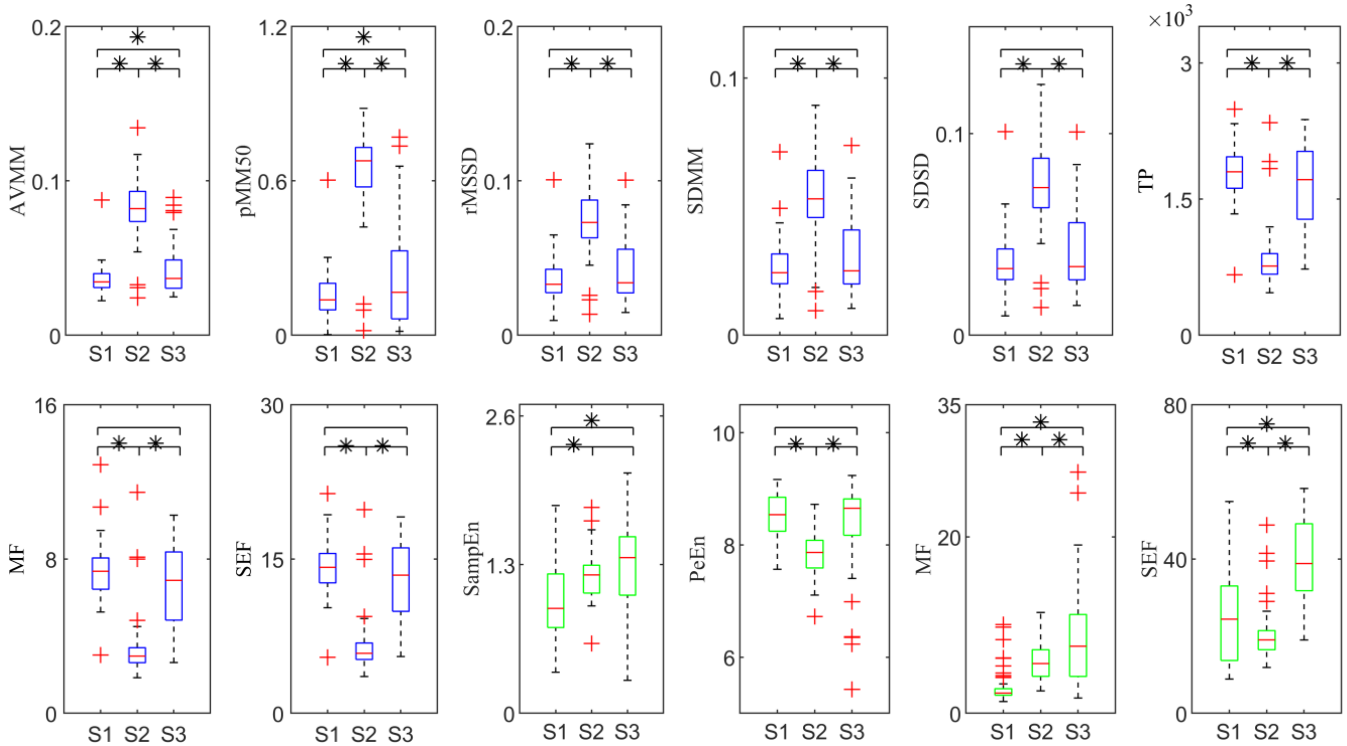


**Figure 8.** The box plots related to the distribution of AVMM, pMM50, rMSSD, SDMM, SDSD, TP, MF, SEF of EEGV (blue box) and SampEn, PeEn, MF, SEF of EEG (green box) corresponding to stage 1 (S1) to stage 3 (S3) from 56 patients. The significant difference giving $p < 0.05$ by Bonferroni correction is marked with asterisk (*).

sampling rates, the mean ICIs are nearly equal to the theoretical values. In special, significant difference is observed among groups of 40 Hz, but no significant difference is observed when removing the group sampled at 64 Hz. Furthermore, errors in ICI measures are related to sampling frequency and is on a downward trend with increase of sampling rate. The error is small if Nyquist-Shannon sampling theorem is satisfied, while sampling at 64 Hz on 40 Hz signal causes an unaccepted error.

To further investigate the stability of proposed EEGV indices with different sampling rates, the original EEG signals sampled at 125 Hz are resampled to 64 Hz, 250 Hz, 500 Hz and 1000 Hz to simulate the recording at different sampling rate. EEGV indices derived from data sampled at 64 Hz, 125 Hz, 250 Hz, 500 Hz and 1000 Hz are calculated. An overlapping sliding window with a fixed size 30 s and a step 5 s is used on EEG recordings. The indices calculated from 1000 Hz signals are considered as the reference, then Pearson correlation coefficients are calculated between the reference and the corresponding indices derived from the variable sampling frequencies. The results are presented in Table 1. Sampling at 125 Hz, 250 Hz or 500 Hz results in excellent correlation and no significant difference, while the decrease is significant at 64 Hz. For this subject, the sampling rate as low as 125 Hz is adequate, but a lower sampling rate (i.e., 64 Hz) may decline the accuracy in calculation of EEGV indices.

### *3.3 Determination of different stages*

Both EEG and EEGV patterns during awake, induction and maintenance, and emergence of general anesthesia are generally different. EEG frequency becomes slower and EEG amplitude becomes larger with increase of anesthetic concentration until the emergence of burst and suppression pattern. In this point of view EEGV amplitude and dispersion were expected to become larger with increase of anesthetic concentration. Whereas the frequency would be expected to become smaller with increase of anesthetic concentration. The AVMM, pMM50, rMSSD, SDMM, SDSD, TP, MF, SEF of EEGV and SampEn, PeEn, MF and SEF of EEG segments corresponding to S1 to S3 are calculated for each recording. SampEn with $m = 2$, $r = 0.2 \times$ standard deviation and PeEn with $m = 6$, $\tau = 1$ are illustrated in previous studies [7, 29, 37]. The box plots related to the distribution of proposed indexes from 56 patients are shown in Figure 8. Changes in AVMM, pMM50, rMSSD, SDMM and SDSD are similar. The AVMM significantly increases from S1 to S2 with induction and loss of consciousness, then significantly decreases during recovery from general anesthesia. The TP, MF, SEF of EEGV and PeEn, SEF of EEG inversely change during different periods of anesthesia. Induction and maintenance of anesthesia significantly decreases TP, and there is a significant increase during emergence. SampEn and MF of EEG cannot correctly separate each state from S1 to S3. Generally, within a short period of time during emergence from general anesthesia, patients gradually regain spontaneous activities and consciousness until to sufficient recovery. It is noted that the EEGV measures AVMM and pMM50 significantly differentiate S1 from S3 in spite of small difference between these two states. Therefore, they have high resolution to represent consciousness level of patients.

### *3.4 Discrimination of awake and unconscious*

To illustrate the discrimination performance between consciousness and unconscious conditions, ROC analysis is used and corresponding AUC is calculated. The performance of proposed method is compared with SampEn, PeEn, MF and SEF of EEG. The gold standard EACL and commercial BIS index are used to label the states of awake and unconscious states. Generally, the BIS index from 40 to 60 indicates an appropriate anesthesia level to ensure a low probability of intraoperative awareness. The value of 60 signifies a threshold for distinguishing consciousness and unconscious. The values of EACL and BIS lower than 60 indicate the unconscious state, and higher than 60 indicate consciousness. Figure 9

**Table 2.** The statistical results of AUC of ROCs from 56 patients for distinguishing the consciousness and unconscious labeled by EACL and BIS index.

| Index | | vs. EACL | vs. BIS |
|---|---|---|---|
| EEGV | AVMM | $0.90 \pm 0.11^{*\dagger\ddagger\ddagger}$ | $0.91 \pm 0.10^{*\dagger\ddagger\ddagger}$ |
| | pMM50 | $0.89 \pm 0.12^{*\dagger\ddagger\ddagger}$ | $0.87 \pm 0.11^{*\ddagger\ddagger}$ |
| | rMSSD | $0.87 \pm 0.12^{*\dagger\ddagger\ddagger}$ | $0.88 \pm 0.11^{*\dagger\ddagger\ddagger}$ |
| | SDMM | $0.87 \pm 0.12^{*\dagger\ddagger\ddagger}$ | $0.89 \pm 0.11^{*\dagger\ddagger\ddagger}$ |
| | SDSD | $0.86 \pm 0.12^{*\dagger\ddagger\ddagger}$ | $0.88 \pm 0.11^{*\dagger\ddagger\ddagger}$ |
| | TP | $0.90 \pm 0.11^{*\dagger\ddagger\ddagger}$ | $0.89 \pm 0.10^{*\dagger\ddagger\ddagger}$ |
| | MF | $0.90 \pm 0.11^{*\dagger\ddagger\ddagger}$ | $0.90 \pm 0.10^{*\dagger\ddagger\ddagger}$ |
| | SEF | $0.90 \pm 0.11^{*\dagger\ddagger\ddagger}$ | $0.91 \pm 0.10^{*\dagger\ddagger\ddagger}$ |
| EEG | SampEn | $0.49 \pm 0.19$ | $0.57 \pm 0.19$ |
| | PeEn | $0.81 \pm 0.16$ | $0.85 \pm 0.14$ |
| | MF | $0.37 \pm 0.16$ | $0.47 \pm 0.19$ |
| | SEF | $0.66 \pm 0.17$ | $0.71 \pm 0.17$ |

The asterisk (*), dagger (†), double asterisk (‡‡) and double dagger (‡) indicate significant difference compared with SampEn, PeEn, MF and SEF of EEG, respectively. ± indicates standard deviation.

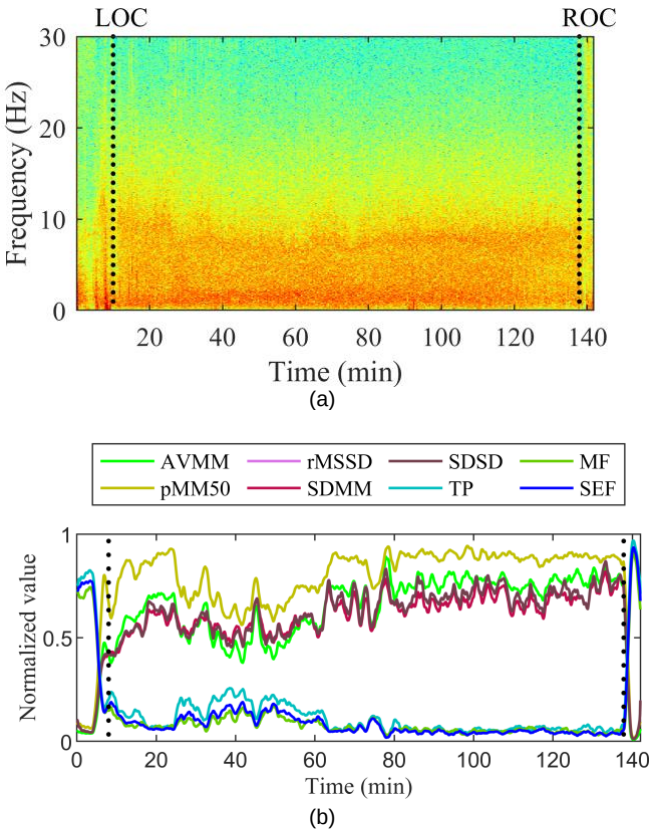


**Figure 10.** The relationship between the EEG variability indexes and the changes of EEG oscillations during general anesthesia. (a) The spectrogram of EEG signal, dark red shows higher spectral power; (b) normalized EEG variability indexes.

shows a case of ROC analysis for EEGV and EEG measures to classify consciousness and unconscious states referring to EACL. The statistical results for AUC of AVMM, pMM50, rMSSD, SDMM, SDSD, TP, MF, SEF of EEGV and SampEn, PeEn, MF, SEF of EEG from 56 patients are shown in table 2. The EEGV derived parameters yield a significant higher AUC

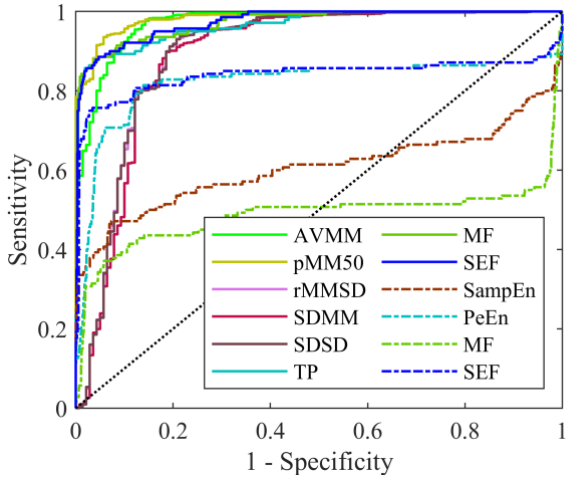


**Figure 9.** ROC curves of different EEGV (solid line) and EEG (dashed line) measures for classifying consciousness and unconscious states of one patient.

**Table 3.** The Pearson's correlation coefficients of AVMM, pMM50, rMSSD, SDMM, SDSD, TP, MF, SEF based on EEGV and SampEn, PeEn, MF and SEF based on EEG versus EACL and BIS from 56 patients.

| | Index | vs. EACL | vs. BIS |
|---|---|---|---|
| EEGV | AVMM | 0.66 ± 0.19$^{*\dagger\ddagger}$ | 0.53 ± 0.33$^{*\ddagger}$ |
| | pMM50 | 0.68 ± 0.19$^{*\dagger\ddagger}$ | 0.49 ± 0.34$^{*\ddagger}$ |
| | rMSSD | 0.54 ± 0.22$^{*\dagger\ddagger}$ | 0.53 ± 0.29$^{*\dagger\ddagger}$ |
| | SDMM | 0.55 ± 0.22$^{*\dagger\ddagger}$ | 0.54 ± 0.29$^{*\dagger\ddagger}$ |
| | SDSD | 0.54 ± 0.22$^{*\dagger\ddagger}$ | 0.53 ± 0.29$^{*\ddagger}$ |
| | TP | 0.70 ± 0.18$^{*\dagger\ddagger}$ | 0.53 ± 0.34$^{*\ddagger}$ |
| | MF | 0.72 ± 0.17$^{*\dagger\ddagger}$ | 0.54 ± 0.35$^{*\ddagger}$ |
| | SEF | 0.71 ± 0.18$^{*\dagger\ddagger}$ | 0.54 ± 0.35$^{*\ddagger}$ |
| EEG | SampEn | - 0.05 ± 0.31 | 0.18 ± 0.26 |
| | PeEn | 0.47 ± 0.28 | 0.48 ± 0.28 |
| | MF | - 0.10 ± 0.29 | 0.13 ± 0.27 |
| | SEF | 0.32 ± 0.31 | 0.32 ± 0.28 |

The asterisk (*), dagger (†), double asterisk (‡) and double dagger (‡) indicate significant difference compared with SampEn, PeEn, MF and SEF of EEG, respectively. ± indicates standard deviation.

in detecting two different states. For instance, AVMM (0.90 ± 0.11) of our proposed method far surpass SampEn (0.49 ± 0.19), PeEn (0.81 ± 0.16), MF (0.37 ± 0.16) and SEF (0.66 ± 0.17) of traditional methods. It is demonstrated that EEGV analysis achieves a better result in all terms compared to existing methods.

### *3.5 Monitoring the consciousness level*

Figure 10 shows the changes of EEG oscillations and EEGV indexes during a general anesthesia. A spectrogram is presented to indicate the changes in frequency content of the EEG as shown in Figure 10 (a). The colours clearly show the alterations in EEG spectral power. The beta (13-30 Hz) rhythms decrease with the loss of consciousness, in contrast, the slow oscillations including alpha (8-12 Hz) and delta (<4 Hz) activity increase. All EEGV indexes can track the changes in consciousness level with increasing anesthetic drug effect as shown in Figure 10 (b). AVMM, pMM50, rMSSD SDMM and SDSD are negatively correlate with high frequency oscillations in EEG, while positively correlate with low frequency oscillations, and vice versa in cases of TP, MF and SEF. As the loss of consciousness, the AVMM, pMM50, rMSSD, SDMM and SDSD increase while TP, MF and SEF decrease.

In order to deepen evaluation of accurately tracking brain states, the trend of AVMM, pMM50, rMSSD, SDMM, SDSD, TP, MF and SEF is confirmed by the correlation versus EACL and BIS, which are used as real state of the patients. The results are also compared with SampEn, PeEn, MF and SEF of EEG. An overlapping sliding window with a fixed size 30 s is used on EEG recordings for monitoring the DOA. The window moves every 5 s to provide synchronous parameter with EACL and BIS sampled at 0.2 Hz. As can be seen in Figures 8 and 10, the range and trend direction are different among parameters. Therefore, linear regression between each parameter and the gold standard (i.e., BIS and EACL) is used as estimates of a unit of measure, to normalize the parameters

value into the range of 0 to100. Subsequently, Pearson's correlation coefficients are calculated as shown in table 3. The EEGV parameters show a higher correlation with both EACL and BIS compared with conventional methods. For instance, we note that AVMM (0.66 ± 0.19) of our proposed method far surpass SampEn (-0.05 ± 0.31), PeEn (0.47 ± 0.28), MF (-0.10 ± 0.29) and SEF (0.32 ± 0.31) of traditional methods. It is demonstrated that the proposed method superior to the traditional methods in accuracy of tracking the level of consciousness.

## 4. Discussion

In this paper, we presented a novel EEGV analysis to assess the variation of EEG signals for deriving reliable DOA monitoring. EEGV was defined by extracted ICIs that measure the time between each quasi-period interval of EEG. Increasing DOA leaded to the predominance of patterns at lower frequencies, often at higher amplitudes underlying EEGV. Both time-domain and frequency-domain parameters of EEGV including AVMM, pMM50, rMSSD, SDMM, SDSD, TP, MF and SEF were employed. The variation behavior of EEG measured by EEGV was found correlated to consciousness level. Various indices have been suggested for similar use of assessing DOA during past couple of decades. In order to investigate the effectiveness of proposed method, the result is also compared to previous methods. The linear features of MF and SEF represent frequency shift of EEG during general anesthesia, the nonlinear features of SampEn and PeEn measure the complexity of EEG. They are all popular and widely used in recent studies. For instance, Liu *et al.* [25] used MF, SEF, SampEn, PeEn and Gu *et al.* [26] used PeEn, SEF as the input of artificial neural network for monitoring DOA. In [29] and [30], SampEn and PeEn were selected as the sub-parameters to train a recurrent neural network and an adaptive neurofuzzy system for estimating DOA. The proposed EEGV derived parameters could discriminate EEG data into different stages during anesthesia in 56 patients with improved performance compared with existing algorithms. Furthermore, the higher correlation with both EACL and BIS demonstrated better performance across all of the patients for predicting DOA. The results indicate that EEGV measuring and the corresponding parameters are an excellent candidate for use in an EEG monitor and would also improve the performance of existing literature of learning-based methods.

From the results, AVMM, pMM50, rMSSD, SDMM and SDSD increase when patients lose their awareness, then decrease with recovery of consciousness. In contrast, the TP, MF and SEF of EEGV decrease with loss of consciousness. General anesthetics primarily act on the neurotransmitter receptors in the CNS for either enhancing inhibitory signals or blocking excitatory signals [32]. The enhanced inhibition makes a significant contribution to inactivating large areas of brain and generate anesthetized state. Similar to HRV analysis reflecting the balance between sympathetic and parasympathetic modulation in human autonomic nervous system, the variability in EEG can reflects the intrinsic balance shift between excitation and inhibition of CNS caused by general anesthesia administration. The AVMM, pMM50, rMSSD, SDMM, SDSD predominantly reflects inhibition activity, and TP, MF, SEF is accompanied by a marked enhance in excitation activation. Moreover, many studies have shown that gamma-aminobutyric acid-mediated sevoflurane, desflurane, or propofol generally caused a decrease in higher EEG gamma (> 30 Hz) and beta (13-30 Hz) rhythms, in contrast, an increase in slow oscillations including alpha (8-12 Hz) and delta (< 4 Hz) activity [38-40]. General anesthesia lengthens the time interval between the periods of EEG activity, that is also one reason for an apparently increases in EEGV amplitude and a reduction in frequency during induction and maintenance as shown in Figure 3. The pMM50, rMSSD, SDMM and SDSD mainly reflect inter-cycle smaller changes in time interval. With the decrease of high frequency contents and increase of low frequency contents in EEG during induction and maintenance of general anesthesia, the histogram of time intervals between local extrema tends to be a broad distribution as shown in Figure 4 (c), and hence causing a higher variance, which is measured by rMSSD, SDMM and SDSD. Furthermore, this frequency shift increases the occurrence of long difference between successive time intervals of local extrema as shown in Figure 5, and thus resulting in increase of pMM50. The pMM50 at selected threshold of 50 ms in successive intervals significantly separated induction and maintenance from awake or emergence. The results would have been very similar even though a value of 30 ms or 40 ms was selected.

It is well known that EEG is very susceptible to artifacts especially in awake and recovery stages. During awake stage, EEG signal is usually contaminated by artifacts such as eye movement, blinks and baseline drift. Furthermore, most researchers avoid head and neck surgery to investigate EEG during anesthesia, because it is difficult to reject artifacts caused by surgical procedure in this type of surgery. The methods with resistance to artifacts would be more favored by researchers and clinicians. SampEn and MF are extremely sensitive to artifacts [25, 41], so they are not feasible to determine different stages of EEG during general anesthesia as presented in Figure 8, because of undesirable decrease in SampEn and MF of EEG caused by blink artifacts and baseline drift during S1 and S3 [25]. PeEn is more robust to noise and artifacts by considering the distribution of ordinal patterns rather than raw amplitude of data [24]. However, all EEGV derived parameters work fine (Figure 8). Different with traditional approaches, EEGV analysis characterizes the behavior of EEG depends on ICI instead of the values themselves, meaning relative rather than absolute magnitude,

so it reduces the bad effect of noise or artifacts and thus improves the accuracy of DOA estimation. The ICI measurement instead of frequency domain analysis is another improvement to responds to rapid changes in EEG signals that result from variations in the brain state. It was approved by the significant improvement of MF and SEF of EEGV compared with that of EEG as shown in Tables 2 and 3. Higher AUC and correlation coefficient values of EEGV analysis also indicate a stronger indicator of DOA during surgery in spite of under noisy environments, which stands up the value of our study.

However, there are some potential limitations of current study. In anesthesia care, balanced general anesthesia is the most common management strategy, which use different drugs together for desired effects [42]. However, the underlying mechanisms of general anesthetic action are different. For instance, ketamine acts at *N*-methyl-d-aspartate glutamate receptors, whereas the primary target of propofol and sevoflurane is gamma-aminobutyric acid A receptor. This difference leads to different EEG changes of general anesthesia. Ketamine, related to propofol and sevoflurane, oppositely increases the beta range rhythms and decrease the delta activity [43]. Various studies show that BIS paradoxically increase after ketamine administration [43-45]. This would require additional larger data set and patients with varying kinds of administered anesthetics for further evaluation of the presented technology.

As we know, the noise or artifacts is a very big and tough problem in EEG measurement. Noise caused misinterpretation of EEG by BIS algorithm is also one of serious drawbacks in BIS system despite having been widely used in daily anesthesia practice. Interferences from several electric devices such as electrocautery equipment, forced-air warming blankets and the otorhinolaryngology positioning system have been reported to cause paradoxical BIS changes [43, 46]. That is why the correlation versus EACL performs better than BIS in our results. In general, the main purpose of preprocessing is to remove noise and artifacts in signals. However, it is a very challenge task due to the weak amplitude, nonlinearity and nonstationarity of EEG signals. Various methods have been proposed to remove the noise and artifacts from EEG data [47]. The classical IIR or FIR filters, and wavelet filters are two widely used techniques. In this paper, a bandpass FIR filter was used to exclude artifacts of less than 0.5 Hz or greater than 47 Hz. But both of them use fixed basis functions (i.e., sine and cosine functions, or wavelet). Empirical mode decomposition (EMD) introduced by Huang et al. [48] adaptively decomposes signals into several intrinsic mode functions (IMF) in order from high to low frequency without any assumed basis functions. So, it highly applies to analysis of nonlinear and nonstationary signals. The filtered EEG can be reconstructed by selected IMFs within special frequency bands of interests. In the future, we will further investigate the reliability of the proposed algorithm on EEG contaminated by different kind of noise and artifacts. Also, we will adjust the preprocessing technique of EEG by using EMD-based filter and further confirm the performance of the proposed method under different combination of IMFs.

Burst suppression (BS) is known as alternating stretches of high amplitude (bursts) and low amplitude (suppression) in EEG during deep anesthesia [49]. With increasing anesthetic drug concentration, SampEn has the ability to distinguish the BS state, but BIS and PeEn may provide incorrect results [30, 50, 51]. Note that all EEG analyzed in this study do not include any BS patterns. Whether the proposed method is robust in the characterization of the BS pattern would need to be further validated.

## 5. Conclusion

The current study is the first one to propose an aperiodic analysis technology of EEG for improvement of determining anesthesia state of patients. In this approach, we first defined the ICI data extracted from EEG to transform raw data to a series of EEGV data. Then time-domain and frequency-domain methods were used to perform EEGV analysis. Compared with traditional techniques, EEGV measures the variation in time intervals between consecutive extreme instead of raw voltage amplitude. It could serve as a new trend to explore DOA monitoring since providing information about the balance between excitation and inhibition. It was validated with patients under general anesthesia that the EEGV derived parameters including AVMM, pMM50, rMSSD, SDMM, SDSD, TP, MF and SEF provided a promising methodology to more precisely differentiate states of consciousness and assess DOA than existing EEG-based parameters. Especially, the spectral features of EEGV can be suggested as the optimal measures for DOA in term of AUC and correlation coefficient for clinical practice. This work has also potential for other EEG-based evaluations such as epilepsy, stroke, Alzheimer's disease, depression, and sleep stage scoring.

## Acknowledgements

## References

[1] P. L. Purdon, E. T. Pierce, E. A. Mukamel et al., "Electroencephalogram signatures of loss and recovery of consciousness from propofol," *Proc. Natl. Acad. Sci. U.S.A.*, vol. 110, no. 12, pp. E1142-E1151, Mar. 2013.

[2] P. S. Sebel, T. A. Bowdle, M. M. Ghoneim et al., "The incidence of awareness during anesthesia: a multicenter united states study," *Anesth. Analg.*, vol. 99, no. 3, pp. 833-839, Sep. 2004.

[3] K. Leslie, M. T. V. Chan, P. S. Myles et al., "Posttraumatic stress disorder in aware patients from the B-aware trial," *Anesth. Analg.*, vol. 110, no. 3, pp. 823-828, Mar. 2010.

[4] M. D. Kertai, N. Pal, B. J. A. Palanca et al., "Association of perioperative risk factors and cumulative duration of low

bispectral index with intermediate-term mortality after cardiac surgery in the B-unaware trial," *Anesthesiology*, vol. 112, no. 5, pp. 1116-1127, Mar. 2010.

[5] T. G. Short, K. Leslie, M. T. V. Chan et al., "Rationale and design of the balanced anesthesia study: a prospective randomized clinical trial of two levels of anesthetic depth on patient outcome after major surgery," *Anesth. Analg.*, vol. 121, no. 2, pp. 357-365, Aug. 2015.

[6] B. Urban, "Current assessment of targets and theories of anaesthesia," *Br. J. Anaesth.*, vol. 89, no. 1, pp. 167-183, Jul. 2002.

[7] Z. Liang, Y. Wang, X. Sun et al., "EEG entropy measures in anesthesia," *Front. Comput. Neurosci.*, vol. 9, no. 16, Feb. 2015.

[8] I. J. Rampil, "A Primer for EEG Signal Processing in Anesthesia," *Anesthesiology*, vol. 89, no. 4, pp. 980-1002, Oct. 1998.

[9] V. Maja, P. Talja, N. Tenkanen et al., "Description of the Entropy™ algorithm as applied in the datex-ohmeda S/5™ entropy module," *Acta Anaesthesiol Scand*, vol. 48, no. 2, pp. 154-161, Feb. 2004.

[10] J. Drummond, C. Brann, D. Perkins et al., "A comparison of median frequency, spectral edge frequency, a frequency band power ratio, total power, and dominance shift in the determination of depth of anesthesia," *Acta Anaesthesiol Scand*, vol. 35, no. 8, pp. 693-699, Nov. 1991.

[11] J. Kortelainen, E. Väyrynen, and T. Seppänen, "Depth of anesthesia during multidrug infusion: separating the effects of propofol and remifentanil using the spectral features of EEG," *IEEE Trans. Biomed. Eng.*, vol. 58, no. 5, pp. 1216-1223, May. 2011.

[12] Q. Liu, Y.-F. Chen, S.-Z. Fan et al., "Improved spectrum analysis in EEG for measure of depth of anesthesia based on phase-rectified signal averaging," *Physiol. Meas.*, vol. 38, no. 2, pp. 116-138, Feb. 2017.

[13] N. Hazarika, T. Ah Chung, and A. A. Sergejew, "Nonlinear considerations in EEG signal classification," *IEEE Trans. Signal Process.*, vol. 45, no. 4, pp. 829-836, Apr. 1997.

[14] X. S. Zhang, R. J. Roy, and E. W. Jensen, "EEG complexity as a measure of depth of anesthesia for patients," *IEEE Trans. Biomed. Eng.*, vol. 48, no. 12, pp. 1424-1433, Dec. 2001.

[15] M. Jospin, P. Caminal, E. W. Jensen et al., "Detrended fluctuation analysis of EEG as a measure of depth of anesthesia," *IEEE Trans. Biomed. Eng.*, vol. 54, no. 5, pp. 840-846, Apr. 2007.

[16] T. Nguyen-Ky, P. Wen, and Y. Li, "An improved detrended moving-average method for monitoring the depth of anesthesia," *IEEE Trans. Biomed. Eng.*, vol. 57, no. 10, pp. 2369-2378, Oct. 2010.

[17] X. Li, F. Wang, and G. Wu, "Monitoring depth of anesthesia using detrended fluctuation analysis based on EEG signals," *J. Med. Biol. Eng.*, vol. 37, no. 2, pp. 171-180, Jan. 2017.

[18] P. Gifani, H. R. Rabiee, M. H. Hashemi et al., "Optimal fractal-scaling analysis of human EEG dynamic for depth of anesthesia quantification," *J. Franklin Inst.*, vol. 344, no. 3, pp. 212-229, 2007.

[19] T. Nguyen-Ky, P. Wen, and Y. Li, "Monitoring the depth of anaesthesia using Hurst exponent and Bayesian methods," *IET Signal Process.*, vol. 8, no. 9, pp. 907-917, Dec. 2014.

[20] K. Hayashi, N. Mukai, and T. Sawa, "Poincaré analysis of the electroencephalogram during sevoflurane anesthesia," *Clin. Neurophysiol.*, vol. 126, no. 2, pp. 404-411, Feb. 2015.

[21] J. Bruhn, H. Röpcke, and A. Hoeft, "Approximate entropy as an electroencephalographic measure of anesthetic drug effect during desflurane anesthesia," *Anesthesiology*, vol. 92, no. 3, pp. 715-726, Mar. 2000.

[22] R. Shalbaf, H. Behnam, J. Sleigh et al., "Measuring the effects of sevoflurane on electroencephalogram using sample entropy," *Acta Anaesthesiol. Scand.*, vol. 56, no. 7, pp. 880-889, Mar. 2012.

[23] Q. Liu, Y.-F. Chen, S.-Z. Fan et al., "EEG signals analysis using multiscale entropy for depth of anesthesia monitoring during surgery through artificial neural networks," *Comput. Math. Methods Med.*, vol. 2015, Sep. 2015, Art. no. 232381.

[24] X. Li, S. Cui, and Logan J. Voss, "Using permutation entropy to measure the electroencephalographic effects of sevoflurane," *Anesthesiology*, vol. 109, no. 3, pp. 448-456, Sep. 2008.

[25] Q. Liu, Y.-F. Chen, S.-Z. Fan et al., "A comparison of five different algorithms for EEG signal analysis in artifacts rejection for monitoring depth of anesthesia," *Biomed. Signal Process. Control*, vol. 25, pp. 24-34, Mar. 2016.

[26] Y. Gu, Z. Liang, and S. Hagihira, "Use of multiple EEG features and artificial neural network to monitor the depth of anesthesia," *Sensors*, vol. 19, no. 11, pp. 2499, May. 2019.

[27] J. S. Richman, and J. R. Moorman, "Physiological time-series analysis using approximate entropy and sample entropy," *Am. J. Physiol. Heart Circ. Physiol.*, vol. 278, no. 6, pp. H2039-H2049, 2000.

[28] C. Bandt, and B. Pompe, "Permutation entropy: a natural complexity measure for time series," *Phys. Rev. Lett.*, vol. 88, no. 17, 2002, Art. no. 174102.

[29] R. Li, Q. Wu, J. Liu et al., "Monitoring depth of anesthesia based on hybrid features and recurrent neural network," *Front. Neurosci.*, vol. 14, Feb. 2020.

[30] A. Shalbaf, M. Saffar, J. W. Sleigh et al., "Monitoring the depth of anesthesia using a new adaptive neurofuzzy system," *IEEE J. Biomed. Health Inform.*, vol. 22, no. 3, pp. 671-677, May. 2017.

[31] C. Orphanidou, and I. Drobnjak, "Quality assessment of ambulatory ECG using wavelet entropy of the HRV signal," *IEEE J. Biomed. Health Inform.*, vol. 21, no. 5, pp. 1216-1223, Sep. 2017.

[32] A. H. Taub, Y. Katz, and I. Lampl, "Cortical balance of excitation and inhibition is regulated by the rate of synaptic activity," *J. Neurosci.*, vol. 33, no. 36, pp. 14359-14368, Sep. 2013.

[33] D. P. Aksenov, L. Li, M. J. Miller et al., "Effects of anesthesia on BOLD signal and neuronal activity in the somatosensory cortex," *J. Cereb. Blood Flow Metab.*, vol. 35, no. 11, pp. 1819-1826, Nov. 2015.

[34] G. J. A. Jiang, S. Z. Fan, M. F. Abbod et al., "Sample entropy analysis of EEG signals via artificial neural networks to model patients' consciousness level based on anesthesiologists experience," *BioMed Res. Int.*, vol. 2015, 2015, Art. no. 343478.

[35] Z. Wu, and N. E. Huang, "A study of the characteristics of white noise using the empirical mode decomposition method," *Proc. Math. Phys. Eng. Sci.*, vol. 460, no. 2046, pp. 1597-1611, Jun. 2004.

[36] E. R. Reshef, N. D. Schiff, and E. N. Brown, "A neurologic examination for anesthesiologists: assessing arousal level during induction, maintenance, and emergence," *Anesthesiology*, vol. 130, no. 3, pp. 462-471, Mar. 2019.
[37] Q. Liu, Y. Chen, S. Fan et al., "Quasi-periodicities detection using phase-rectified signal averaging in EEG signals as a depth of anesthesia monitor," *IEEE Trans. Neural Syst. Rehabil. Eng.*, vol. 25, no. 10, pp. 1773-1784, Oct. 2017.
[38] E. N. Brown, R. Lydic, and N. D. Schiff, "General anesthesia, sleep, and coma," *N Engl J Med*, vol. 363, no. 27, pp. 2638-2650, Dec. 2010.
[39] G. Plourde, and F. Arseneau, "Attenuation of high-frequency (30–200 Hz) thalamocortical EEG rhythms as correlate of anaesthetic action: evidence from dexmedetomidine," *Br. J. Anaesth*., vol. 119, no. 6, pp. 1150-1160, Oct. 2017.
[40] Y. Li, W. Shi, Z. Liu et al., "Effective brain state estimation during propofol-induced sedation using advanced EEG microstate spectral analysis," *IEEE J. Biomed. Health Inform.*, pp. 1-1, Jul. 2020.
[41] R. Shalbaf, H. Behnam, J. W. Sleigh et al., "Monitoring the depth of anesthesia using entropy features and an artificial neural network," *J. Neurosci. Methods*, vol. 218, no. 1, pp. 17-24, Aug. 2013.
[42] E. N. Brown, K. J. Pavone, and M. Naranjo, "Multimodal general anesthesia: theory and practice," *Anesth. Analg.*, vol. 127, no. 5, pp. 1246-1258, Nov. 2018.
[43] A. A. Dahaba, "Different conditions that could result in the Bispectral Index indicating an incorrect hypnotic state," *Anesth. Analg.*, vol. 101, no. 3, pp. 765-773, Sep. 2005.
[44] P. Hans, P.-Y. Dewandre, J. F. Brichant et al., "Comparative effects of ketamine on Bispectral Index and spectral entropy of the electroencephalogram under sevoflurane anaesthesia," *Br. J. Anaesth.*, vol. 94, no. 3, pp. 336-340, Mar. 2005.
[45] H. E. M. Vereecke, M. M. R. F. Struys, and E. P. Mortier, "A comparison of bispectral index and ARX-derived auditory evoked potential index in measuring the clinical interaction between ketamine and propofol anaesthesia," *Anaesthesia*, vol. 58, no. 10, pp. 957-961, Oct. 2003.
[46] M. T. V. Chan, S. S. Ho, and T. Gin, "Performance of the Bispectral Index during electrocautery," *J. Neurosurg. Anesthesiol.*, vol. 24, no. 1, pp. 9-13, Jan. 2012.
[47] X. Jiang, G. B. Bian, and Z. Tian, "Removal of artifacts from EEG signals: a review," *Sensors*, vol. 19, no. 5, pp. 987, 2019.
[48] N. E. Huang, Z. Shen, S. R. Long et al., "The empirical mode decomposition and the hilbert spectrum for nonlinear and non-stationary time series analysis," *Proc. R. Soc. Lond. A.*, vol. 454, no. 1971, pp. 903-995, Mar. 1998.
[49] S. Ching, P. L. Purdon, S. Vijayan et al., "A neurophysiological-metabolic model for burst suppression," *Proc. Natl. Acad. Sci. U.S.A.*, vol. 109, no. 8, pp. 3095-3100, Feb. 2012.
[50] R. Shalbaf, H. Behnam, and H. Jelveh Moghadam, "Monitoring depth of anesthesia using combination of EEG measure and hemodynamic variables," *Cogn. Neurodyn.*, vol. 9, no. 1, pp. 41-51, Feb. 2015.
[51] D. Li, X. Li, Z. Liang et al., "Multiscale permutation entropy analysis of EEG recordings during sevoflurane anesthesia," *J. Neural Eng.*, vol. 7, no. 4, Aug. 2010, Art. no. 046010.